

# Remote Sensing and GIS Based Assessment of Urban Heat Island Pattern in Kaduna Metropolis

Abdu Yaro, Lawal Abdulrashid, Jerome Ayodele John and Yahaya Sani

- Department of Geography, Umaru Musa Yar'adua University, Katsina State. Nigeria

## Abstract

This study examines the pattern and distribution of heat island in Kaduna metropolis based on Landsat Imageries of 1995, 2005 and 2015, whose spatial resolution is sufficient for measurement of some important environmental parameters. The study first identified patterns of land cover changes between the periods and investigated their relationship with Land surface temperature (LST) was established based on Environmental Criticality Index (ECI). Land surface temperature (LST) was retrieved using the mono-window algorithm with area of UHI identified in the study area. Results show that Kaduna city's urban heat island effect is on the increase, substantial and in variance, which could be visually characterized by the spatial pattern of retrieved thermal properties. The study, therefore, concluded that different Land Use Land Cover (LULC) revealed varying temperature, and identified UHI was apparent and more conspicuous in the 2015 as compared to 1995 and 2005 within the metropolis. Particularly, due to the scarcity of vegetation, some hotspots are built-up areas, bare surfaces, central business districts (CBD) areas, and the surface temperature of which is even slightly higher than suburbs. This study suggested a strict adherence to Kaduna master plan, vegetation regeneration and establishment of green areas and parks (go-green initiatives), reflective roofing materials, and lightening of pavements as adaptive/mitigation measures against UHI in the study area.

*Index Terms*- Anthropogenic forces, LULC, Land Surface Temperature, Remote Sensing/GIS, Urban Heat Island

## I. INTRODUCTION

The population will continue to grow in the urban areas of less developed regions, averaging 2.4 percent per year during 2002–2030, consistent with a doubling time of 29 years (UNPD, 2014). The concentration of population in cities is expected to continue such that by 2030, 84 percent of the inhabitants of more developed countries will be urban dwellers. The United Nations (UN) predicts that between 2011 and 2050, the world population is expected to increase by 2.3 billion, increasing from 7.0 billion to 9.3 billion (UN, World Urbanization Prospects: 2011). At the same time, the population living in urban areas is projected to increase by 2.6 billion, from 3.6 billion in 2011 to 6.3 billion by 2050 (UNPD, 2011). Thus, the urban areas of the world are expected to absorb all the population growth over the next four decades while at the same time drawing in some of the rural population such that nearly all the population growth (64%) will be in the cities of developing countries. With the estimated population of 167 million (NPC, 2014), Nigeria is experiencing one of the most unprecedented rates of urbanization worldwide. The country now has 36 states including the FCT and 774 Local Government Councils. The national average urban growth rate is about 11% with the minimum of over 5.3% per annum. Some individual cities have higher urban growth rates than the national average. Kaduna, for example, is growing at 11.5%, Port Harcourt 10.5% while Lagos has an estimated growth rate of between 10% and 15% yearly (NITP, 2011).

Human activities especially in urban areas are becoming more technologically advanced leading to changes in land use/land cover pattern. Urbanization which inevitably, results into loss and /or gain of some particular LULC types, remain a critical concern. Unfortunately, both LULC types losing and gaining are contributing to carbon dioxide build-up, atmospheric pollutants as well as anthropogenic heat emission sources (Anup, 2013). However, inadequate proper monitoring of human activities has led to fast changes in LULC beyond physical planning in most metropolitan cities and with no detailed database on LULC making it difficult for proper estimation of the emissions from the different LULC types (Ifatimehin and Ufuah, 2007).

A typical example, in Kaduna metropolis, the unstructured and densely packed Kawo transportation nodes, Kaduna-Abuja expressway, Ahmadu Bello way/Kaduna central market, mechanic village, Rigassa district, with much inadequate regulated commercial activities leading to huge heat emissions, chimney fumes, human and animal respiration, and heat and moisture escape from houses. These emissions lead to the warming of Kaduna metropolis higher than the surrounding rural areas (Zaharaddeen, Ibrahim, and Zachariah, 2016). The pollutants and gases (such as,  $\text{CO}_2$ ) emitted by human activities creates an atmospheric blanket preventing long-wave radiation from escaping into the outer space. The vegetal cover acting as carbon sink is being lost because of urban growth and development. Almost all the green surfaces in the study area are replaced with gray surface with no plan for replanting (Al-Amin, 2005, Aliyu, Garba and Al-Amin, 2014).

Studies revealed that the study of urban heat island effect have gained much importance across the world, due to rapid urbanization, industrialization and population increase (Penget *et al.*, 2012). In Nigeria, several researchers have investigated the pattern and intensity of UHI in some major cities (Umar and Kumar, 2014; Odunuga and Badru, 2015) and concluded that the dynamics of land use land cover (LULC) can influence the pattern of atmospheric and LST which thus can bring about thermal stress. The use of remotely sensed data has been widely applied as a tool to effectively study the influence of urban LULC dynamics on SUHI across the world (Balogun *et al.*, 2012,). Most studies rely on land surface temperatures derived from remotely sensed data as opposed to the traditional methods of measuring the UHI which involved comparison of temperature data from in-situ urban and non-urban meteorological stations (Fujibe, 2009) or by collecting temperature data by transecting between an urban and non-urban area (Akinbode *et al.*, 2008). Studies have shown that remotely sensed LST can provide a spatially continuous data over a whole city or region, permitting visualization of spatial relationships between temperature patterns and urban land use including infrastructural features (Zhang, Wang and Li, 2006, Balogun *et al.*, 2012,).

Studies on the assessment of patterns and distribution of urban heat island (UHI) in Kaduna south and north LGA of Kaduna metropolis, Nigeria, are however scarce if not unavailable. The fundamental objective of this paper is to provide an insight into the dynamics of land cover pattern and its influence on the LST and UHI in north and south LGA of the metropolis. This paper focus on the LST component of the UHI effect, this is due to the fact that UHI is related to the spatial distribution of LST. As a result, LST and UHI are often used interchangeably in this research. Being an important contributor to the UHI effect, it is, therefore, critical to obtain LST as a first and key step to the UHI analysis.

## 2.0 STUDY AREA

The study area is the capital of Kaduna state which is located between latitude  $9^{\circ}\text{N}$  and  $12^{\circ}\text{N}$  of the equator and longitude  $6^{\circ}\text{E}$  and  $9^{\circ}\text{E}$  of the prime meridian and covers a land area of over 43, 460  $\text{km}^2$ . Its natural sphere of influence covers approximately 122 km east to west and 80-96km north to south. The general area on which Kaduna is located was secured in 1902 by a colonial proclamation when the area was declared an administrative station, after the occupation of Northern Nigeria by the British. Generally, the topography of the environment is an undulating terrain of about 700 metres above sea level on the average (Obasanjo, 2015). The Kaduna River is the major river that flows in the area.

The highest temperatures for Kaduna are recorded in April and the range is between 35°C and 41°C, the lowest temperatures are recorded in January and range between 7°C and 13°C, when the cold harmattan winds are fierce and dominate the region generally and In its natural state this zone is supposed to have slightly thick woodland and tall grasses. It is expected to have a continuous cover of well-developed trees some 8-15 metres tall. However, the vegetation in this zone has been modified over the centuries by urbanisation, intense cultivation, grazing and burning. This vegetation zone is therefore now classified as open and park-like grassland (Obasanjo, 2015). The 1991 population census figure for Kaduna was 1,076,283 and this consisted of Kaduna North, Kaduna South and part of Igabi and Chikun Local Government Areas (FGN 2009cs). The 2006 census figure for Kaduna Metropolis was estimated at 1,570,331 (Federal Republic of Nigeria, 2009b). By 2018 the city is expected to have 2,219,327 people inhabitants (NPC, 2015)

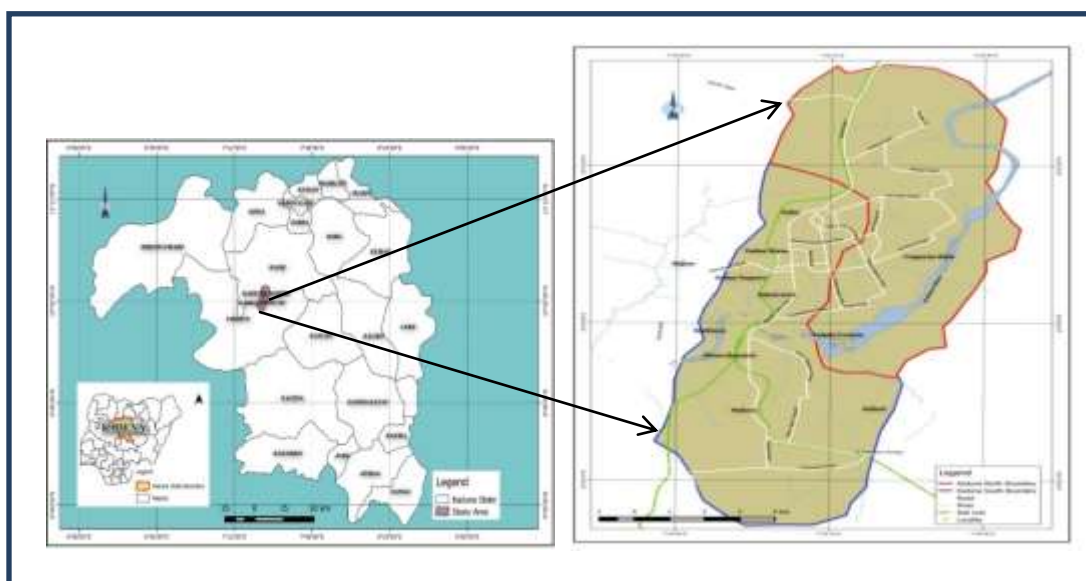


**Figure 1: Location of the Study Area**

Source: GIS Laboratory, Umaru Musa Yar'adua University, 2016

### 3.0 MATERIALS AND METHODS

#### 3.1 DATA

The satellite data used in this study were collected through the United State Geological Survey (USGS), website: ([URL:http://edcns17.cr.usgs.gov/NewEarthExplorer/](http://edcns17.cr.usgs.gov/NewEarthExplorer/)), their spectral and spatial characteristics as well as acquisition dates are shown in Table 1 below:

**Table 1: Details of selected imageries**

Satellite (Sensor)	Row/Path	Date of Acquisition	Source	Resolution	Cloud Cover	Bands Comb. (LULC)	Bands Comb. (NDVI)	Bands Comb. (LST)
Landsat-5 (TM)	53/189	Feb., 4, 1995	USGS	VINR-30 TR- 60	0	5,4,3	4 & 3	6
Landsat-7 (ETM+)	53/189	March, 13, 2005	USGS	VINR-30 TR- 60	0	5,4,3	4 & 3	6
Landsat-8 (OLI/TIRS)	53/189	Feb., 24, 2015	USGS	VINR-30 TR- 60	0	6,5,4	5 & 4	10

Source: USGS (Landsat), 2015

### 3.2 METHODS

For the purpose of this research the mono-window algorithm method was adopted to retrieve the LST from the thermal infra-red band of the Landsat TM, ETM+ and OLI imageries. The method adopted for the study is presented in Fig 3.1 below;

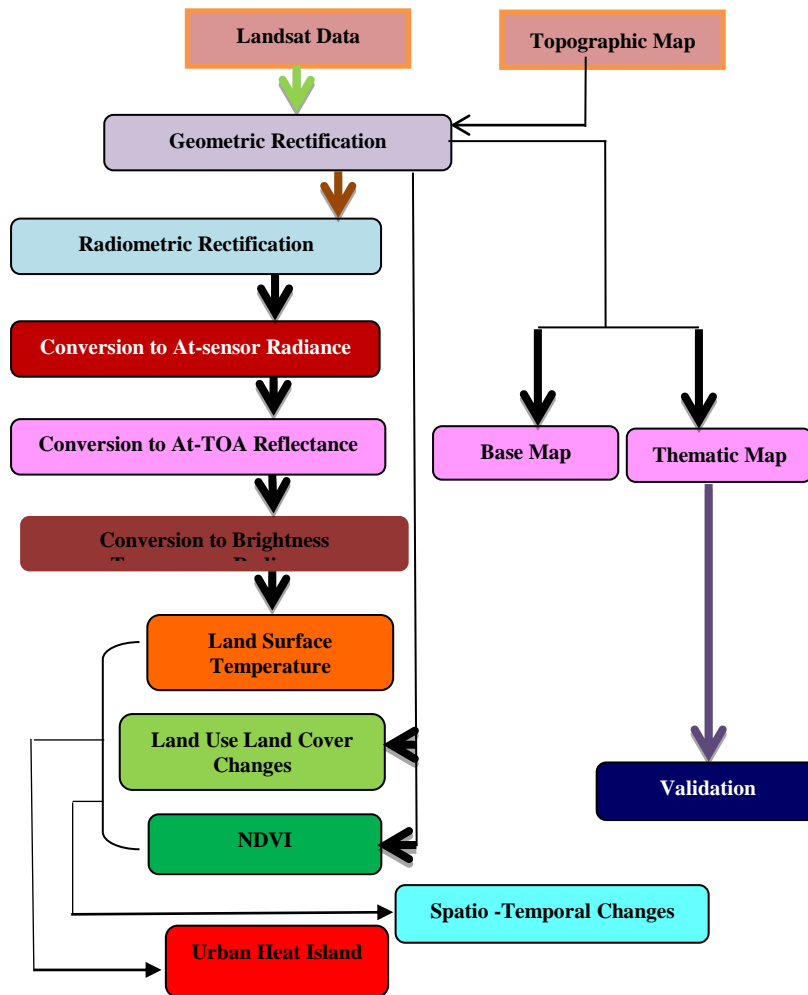


Figure 2: Process Flow of Estimating Surface Temperature and UHI  
Source: Adopted & Modified After Umar and Kumar, 2014

**Land Cover Classifications:** The maximum likelihood classifier scheme was adopted for this research. Based on the prior knowledge of the land cover types in the study area, a chosen color composite (RGB= 432) was used for digitizing polygons around each training site for similar land cover. Then a unique identifier was assigned to each known land cover type. Afterwards, the statistical characterizations (i.e., signatures) of each land cover class were developed. Each composed image was ordered into 5 area classes: water bodies, vegetation, built up areas, bare surface and rock outcrop as shown in Figure 4.

**Image Processing:** All the images were geometrically rectified to WGS1984 Universal Transverse Mercator (UTM) projection and radiometrically corrected before the calculation to avoid a data set specific result. In terms of atmospheric correction, the digital numbers (DN) of the ETM+ image were converted to normalized atmospheric reflectance using the equations below. The calibration parameters can be retrieved from the image head files and the NASA website.

$$L_{\lambda} = gain \times DN + bias$$

$$\text{Expanded version: } L_{\lambda} = 0.0370588 \times DN + 3.2 \dots \dots \dots 1$$

**Where;**

0.0370588=Gain and 3.2=Bias

*L<sub>λ</sub> is the normalized atmospheric reflectance at a particular wavelength.*

### Calculating Reflectance

To convert Landsat radiance values into reflectance (at satellite) values, using the formula as expressed below;

$$R_{\text{sensor}} = (\pi \cdot L_{\lambda} \cdot d^2) / (ESUN_i \cdot \cos(z)) \dots \dots \dots 2$$

Where,

$\pi = 3.14159$ ,

$R_{\text{sensor}}$  is the reflectance at the sensor,  $L_{\lambda}$  is the spectral radiance at the sensor's aperture;  $ESUN_i$  is the mean solar exo-atmospheric irradiance of each band,  $i$ ;  $z$  is the solar zenith angle (zenith angle = 90 – solar elevation angle), which is within the header file; and  $d$  is the earth-sun distance, in astronomical units, which is calculated using the follow EXCEL equation (Eva and Lambin, 1998):

$$d = (1 - 0.01672 \cdot \cos(\text{RADIANS}(0.9856 \cdot (\text{Julian Day} - 4)))) \dots \dots \dots 3$$

### Conversion of Digital Number (DN) to AT-Spectral Radiance

Conversion to spectral radiance is necessary to correct atmospheric effect on the reflectance value; absorption and scattering create an overall effect of “haziness” which reduces the contrast in the image. Calculation of at-sensor spectral radiance is the fundamental step in converting image data from multiple sensors and platforms into a physically meaningful common radiometric scale. Radiometric calibration of the MSS, TM, ETM+, and OLI sensors involves resealing the raw digital numbers ( $Q$ ) transmitted from the satellite to calibrated digital numbers ( $Q_{\text{cal}}$ ), which have the same radiometric scaling for all scenes processed on the ground for a specific period

$$\text{Radiance} = L_{\text{MIN}} + \left( \frac{L_{\text{MAX}} - L_{\text{MIN}}}{Q_{\text{CALMAX}} - Q_{\text{CALMIN}}} \right) \times (Q_{\text{CAL}} - Q_{\text{CALMIN}}) \dots \dots \dots 4$$

**Where;**

**Radiance** = Spectral Radiance at the sensor's aperture in watts/(meter squared \* ster \*  $\mu\text{m}$ ) (Watts /  $\text{m}^2 \cdot \text{ster} \cdot \mu\text{m}$ ),

$L_{\text{MIN}}$  = the spectral radiance that is scaled to  $Q_{\text{CALMIN}}$  in watts/ (meter squared \* ster \*  $\mu\text{m}$ ) (minimum spectral radiance at  $Q_{\text{CAL}}$ )

$L_{\text{MAX}}$  = the spectral radiance that is scaled to  $Q_{\text{CALMAX}}$  in watts/(meter squared \* ster \*  $\mu\text{m}$ ) (maximum spectral radiance at  $Q_{\text{CAL}}$ )

$Q_{\text{CALMAX}}$  = the maximum quantized calibrated pixel value (corresponding to  $L_{\text{MAX}\lambda}$ ) in DN 255

$Q_{\text{CALMIN}}$  = the minimum quantized calibrated pixel value (corresponding to  $L_{\text{MIN}\lambda}$ ) in DN 0 (sometimes 1)

$Q_{\text{CAL}}$  = the quantized calibrated pixel value in DN (Digital Number (DN))

The OLI images which have a different sensor were processed in units of absolute radiance using 32-bit floating point calculations. These values are then converted to 16-bit integer values in the finished level 1 product. These values were then converted to spectral radiance using the radiance scaling factors provided in the metadata file:

$$L\lambda = ML * Qcal + AL \dots \dots \dots 5$$

Where;

$L\lambda$  = Spectral radiance (W/(m<sup>2</sup> \* sr \* μm))

$ML$  = Radiance multiplicative scaling factor for the band (RADIANCE\_MULT\_BAND\_n from the metadata).

$AL$  = Radiance additive scaling factor for the band (RADIANCE\_ADD\_BAND\_n from the metadata).

$Qcal$  = Level 1 pixel value in DN

**Conversion to AT Reflectance**

$$R\lambda = \frac{\pi \times L\lambda \times d2}{ESun\lambda \times \sin(SE)} \dots \dots \dots 6$$

Where;  $R\lambda$ = At surface reflectance,  $L\lambda$ = Spectral radiance,  $\pi$ = 3.142 (constant),  $ESun\lambda$ =Sun elevation angle,  $d2$  = earth-sun distance

Similar to the conversion to radiance, the 16-bit integer values in the level 1 product were also converted to Top of Atmosphere (TOA) reflectance in OLI imagery. The following equation was used to convert level 1 DN values to TOA reflectance:

$$\rho\lambda' = Mp * Qcal + Ap \dots \dots \dots 7$$

Where;

$\rho\lambda'$  = Top-of-Atmosphere Planetary Spectral Reflectance, without correction for solar angle. (Unit less)

$Mp$  = Reflectance multiplicative scaling factor for the band (REFLECTANCE\_W\_MULT\_BAND\_n from the metadata).

$Ap$  = Reflectance additive scaling factor for the band (REFLECTANCE\_ADD\_BAND\_N from the metadata).

$Qcal$  = Level 1 pixel value in DN

**Conversion from Radiance to Brightness Temperature (in degree Celsius)**

TIRS data, TM and ETM+ Band 6 imagery were converted from spectral radiance to a more physically useful variable. This is the effective at-satellite temperatures of the viewed Earth-atmosphere system under an assumption of unity emissivity and using pre-launch calibration constants listed in Table 3.1 below. The conversion formula is:

Equation as;

$$T = \frac{K2}{\ln \left( \frac{K1}{L\lambda} + 1 \right)} \dots \dots \dots 8$$

Where;

$T$  =Temperature [Celsius degree]

$K1$  =Calibration constant 1 [W/(m<sup>2</sup>sr μm)]

$K2$  =Calibration constant 2 [Kelvin]

$ln$ =Natural logarithm

$L\lambda$ =Spectral radiance at the sensor's aperture [W/(m<sup>2</sup>sr μm)]

**Table 2: ETM+ and TM Thermal Band Calibration Constants**

<b>ETM+ and TM Thermal Band Calibration Constants</b>
---

	Constant 1- <b>K1</b> watts/(meter squared * ster * μm)	Constant 2 - <b>K2</b> Kelvin
Landsat 7	666.09	1282.71
Landsat 5	607.76	1260.56

Source: Landsat 8 (L8) Data Users Handbook, 2015

**Estimation of Land Surface Emissivity (LSE)**

In estimating LSE, Normalized Differential Vegetative Index (NDVI) was utilized for emissivity correction;

$$LSE = 0.004P_v + 0.986 \dots\dots\dots 9$$

$$P_v = \left( \frac{NDVI - NDVI_{min}}{NDVI_{max} - NDVI_{min}} \right)^2 \dots\dots\dots 10$$

$$NDVI = \left( \frac{NIR - RED}{NIR + RED} \right) \dots\dots\dots 11$$

Where

**P<sub>v</sub>**= Proportion of vegetation; **NIR**= Near InfraRed Band; **Red**= Red Band; **NDVI<sub>min</sub>**= Minimum value of NDVI; **NDVI<sub>max</sub>**= Maximum value of NDVI

**Estimating Land Surface Temperature**

$$LST = \frac{BT}{1+w} \times \frac{BT}{p} \times \ln(e) \dots\dots\dots 12$$

Where; **BT** = At-sensor brightness temperature; **w** = wavelength of emitted radiance; **p**=  $h \times \frac{c}{s} (1.438 \times 10^{-2} mK)$ ; **h** = Plank’s constant ( $6.626 \times 10^{-34} Js$ ); **s** = Boltzmann constant ( $1.38 \times 10^{-23} J / K$ ); **c** = velocity of light ( $2.998 \times 10^8 m/ s$ ); **e** = LSE

**4.0 RESULTS AND DISCUSSION**

**LandUse LandCover Change Detection**

Based on the supervised classification of the Landsat imageries, the land cover was classified into five categories; namely, vegetation, water bodies, built-up areas, bare surface and rock out-crop. Statistics show that as at 1995, Vegetation and Built up areas constitutes the largest LULC categories in Kaduna metropolis. They collectively occupy an area of 994.40 km<sup>2</sup>, representing 83.20% of the total land cover of the study area. The rock out-crops are the least land cover type. It occupied an area of 13.96 km<sup>2</sup> which represents 1.14% of the total land cover of the study area. Observations from year 2005 show a significant increase in the built areas from 211.40 km<sup>2</sup> in 1995 to 309.50 km<sup>2</sup> in 2005 which implies an increase from 17.69% to 26.00%. Whereas, vegetation land decreases from 65.51% to 45.08% while bare-surface increased from 9.03% to 18.89%. Also between 2005 and 2015, built up areas has the highest rate of expansion from 309.50 km<sup>2</sup> (26.00%) to 436.50 km<sup>2</sup> (36.52%) while there were loss of vegetation and bare surface.

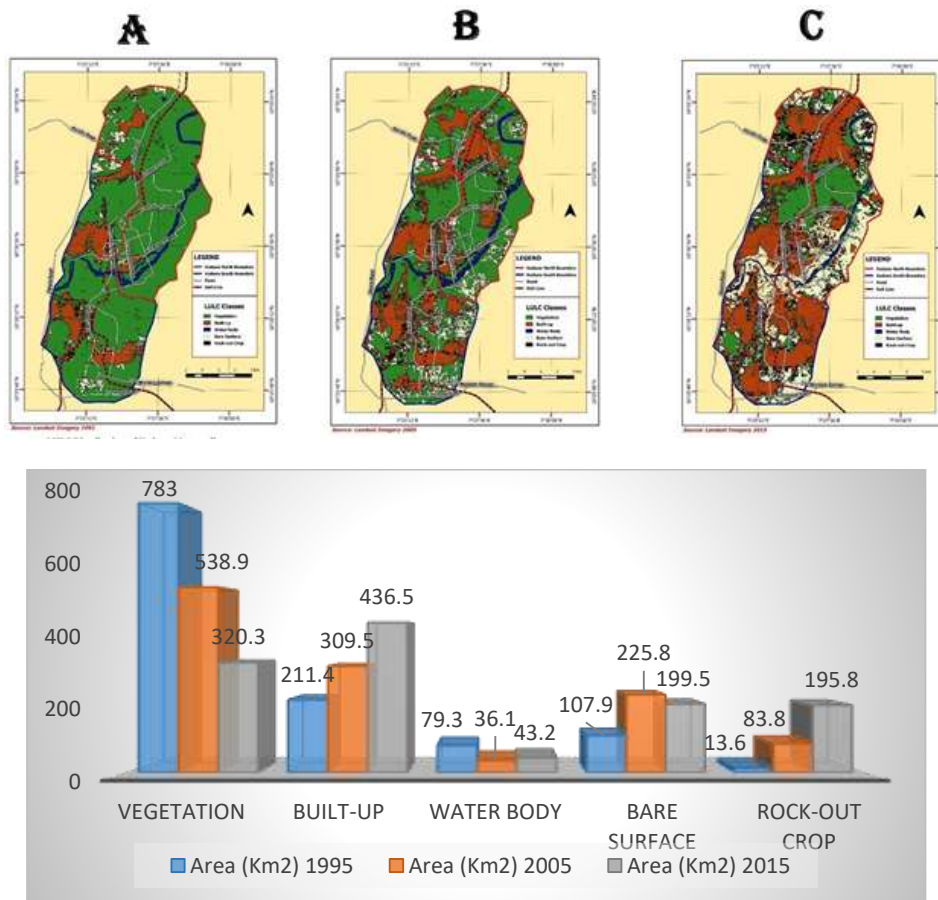


**Figure 3 (i & ii): Land cover categories of study area in comparison (a) 1995, (b) 2015 and (c) 2015**  
 Source: Authors Interpretation of Landsat Imagery, 2015

**Change Detection in Vegetation Density (NDVI)**

The normalized difference vegetation index (NDVI) is a simple graphical or numerical indicator that can be used to analyze the visible and near-infrared bands of the electromagnetic spectrum, and is adopted to analyze remote sensing measurements. Calculations of NDVI for a given pixel always result in a number that ranges from minus one (-1); however, no green leaves give a value close to zero. A zero means no vegetation and close to +1 (0.8 – 0.9) indicates the highest possible density of green leaves. It is observed that lower NDVI corresponds to the built up areas and bare surfaces while high NDVI values corresponds to the less developed natural surfaces as presented in the figure 4 (a, b and c) below. 1995 has the highest NDVI value while 2015 has the lowest which indicates that the NDVI decreases with the urban spreading out.





**Figure 4: Distribution of NDVI of Study Area for (a) 1995, (b) 2005 and (c) 2015**  
*Source: Landsat Imagery, 2015*

### Spatial and Temporal pattern of LST in Kaduna metropolis (1995 – 2015)

Spatial distribution of Land surface temperature (LST) was analyzed in this study in order to detect the extent, temporal pattern and distribution of urban heat island (UHI). The spatial-temporal distributions of LST changes over Kaduna in the three examined dates, The LST was categorized into 5 classes ranging from  $<25 - 27.7^{\circ}\text{C}$  in the surrounding districts to  $32 - 37.9^{\circ}\text{C}$  in the central area and extreme temperature of  $38 - 41.9^{\circ}\text{C}$  was discovered in 2015. The hot spots clustered in high-density residential areas, built-up areas of the urban centre, business axis, and motor park of Kakuri, Barnawa, Nasarawa, UnguwanPama, and Sabon-tasha axis of the southern area and commercial hubs of Ahmadu Bello way, transportation nodes such as the Kawo district area, independence way to Ali Akilu Way, all on the northern axis and at the mechanic village along Kaduna-Abuja bypass (Rigassa and Riga chukun).

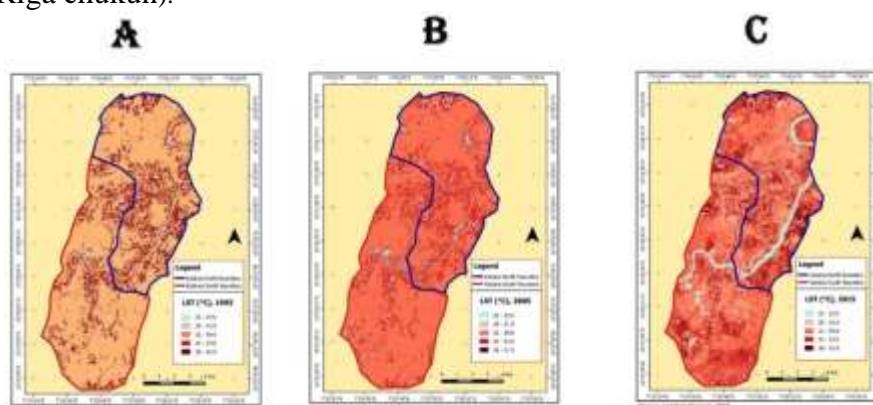


**Figure 5: Distribution of LST of Study Area in comparison (a) 1995, (b) 2005 and (c) 2015**  
*Source: Landsat Imagery, 2015*

**Table 3: Spatial and temporal Distribution of LST (1995 –2015)**

Temperature ( $^{\circ}\text{C}$ )	Area 1995 ( $\text{KM}^2$ )	Area 2005 ( $\text{KM}^2$ )	Area 2015 ( $\text{KM}^2$ )	Change ( $\text{KM}^2$ ) (2015-1995)
$<25-27.9$	311.4	126.6	297.7	-13.7
$28-31.9$	683.0	366.6	575.4	-107.6
$32-34.9$	167.9	489.3	144.3	-23.6
$35-37.9$	29.3	198.5	139.6	110.3
$38-41.9>$	3.6	14.2	38.2	34.6
<b>Total</b>	<b>1195.2</b>	<b>1195.2</b>	<b>1195.2</b>	<b>0</b>

*Source: Author's interpretation of Landsat Imagery, 2015*

Physical ground survey (truth verification) of the study area and by visually inspecting the LST maps, it was further observed that UHI in the study area was having less spatial extent in 1995 compared with that of 2005 and is higher in 2015 (Fig. 5 a, b, c). In the urbanized boundary of the study area in 1995, a relatively small and negligible UHI was observed in the central area (Kurmin Masha, Malili, Cabala Costain/Doki, shooting range, Unguwan Rimi in the northern part of the river and Barnawa, Nasarawa, Sabon Tasha, etc., in the southern part). In 2005, parallel to the increase in the urbanized area, the UHI has also increased and several

UHI spots were discovered over the city. In the year 2015, due to the significant increase in the urbanized area of study area, urban boundaries have been extended and a great amount of bare land and agricultural areas have been converted to urbanized areas.

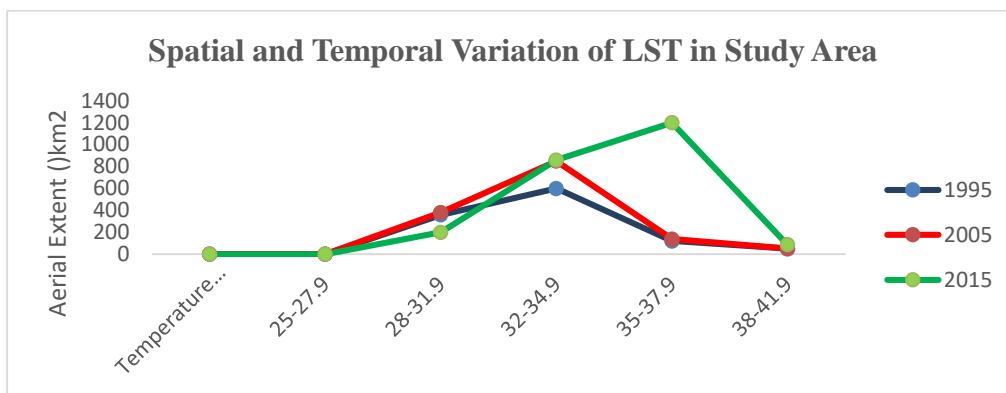


Figure 6: Spatial and Temporal Variation of LST in the Study Area

### Relationship between Land Surface Temperature and LULC

The relationship between LST and land use land cover was derived by calculating the environmental criticality index (ECI). LST vary over the study years across the 5 different LULC types (Figure 7). Overlaying the LST map on the LULC of the study area, the mean surface temperature variation over different land cover types revealed that the majority of the bare surface and impervious surface areas of the study area had temperatures between 32°C and 34.9°C in both 1995 and 2015 in which by implication of the ECI interpretation corresponding to high temperature. And in 2005, however, vegetation and water bodies have similar temperature variations between <28°C and 31.9°C in the study period (1995). By relating the land surface temperature and land use parameter using the Environmental Criticality Index (ECI), it has been found that, LST has very low negative relationship with vegetation cover. The relationship is also insignificant as most of the buildup area fall with low criticality to non-criticality category.

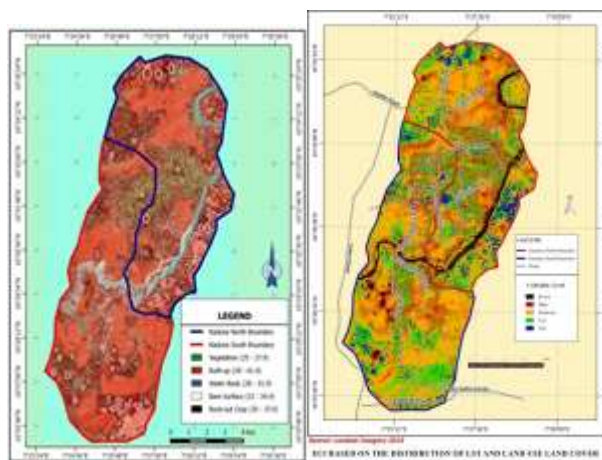


Figure 7: Overlay LST with LULC map and Environmental Criticality index based on LST and Land use/land cover (2015)

Source: Classified from Landsat Imagery, 2015

### 5.0 CONCLUSION AND RECOMMENDATIONS

The pattern and distributions of urban heat island in Kaduna Metropolis have been investigated and results reveal a significant impact of increasing density of the build-up area on land surface temperature. Kaduna city's

urban heat island effect is on the increase, substantial and in variance. The research also established that, most areas having lower temperature in 1995 were converted to hot spots in 2005 and hotter in 2015, due to the increased in build-up areas over the years and corresponding decrease in vegetation (Table 3). This signifies that, changing land use land cover may induce changes in UHI of an area. It went further to establish the relationship between LULC and land surface temperature in the city. The study also promote the use of remote sensing data with GIS technique's for indicating urban surface temperature differences in urban areas with respect to land cover types. It has shown that the surface temperature of the urban environment of Kaduna north and south has been increasing due to anthropogenic influence on the land use & land Cover.

Based on the study, it is recommended that Appraising LST and UHI is of significance to any city since it addresses the issue of human discomfort, thus, a strict adherence to Kaduna master plan, vegetation regeneration and establishment of green areas and parks (go-green initiatives), reflective roofing materials, and lightening of pavements as adaptive/mitigation measures against UHI in the study areas is very paramount.

## REFERENCES

- Akinbode, O. M., Eludoyin, A. O., Fasae, O. A., (2008). Temperature and Relative Humidity Distributions in a Medium-size Administrative Town in Southwest Nigeria. *Journal of Environmental Management*, 87, 95-105.
- Aliyu D.G., and Al-Amin M, (2014). Urban Vegetation Study of Kaduna Metropolis using GIS and Remotely sensed Data, *Journal of Natural Sciences Research*, ISSN 2225-0921 (Online) Vol.4, No.2, 2014
- Anup, S. (2013, November 11). Climate Change and Global Warming Introduction. Retrieved from Global Issues: <http://www.globalissues.org/article/233/climate-change-and-global-warming-introduction#globalissues-org>
- Balogun A.A, Balogun I.A, Adefisan A.E, Abatan A.A (2009). Observed characteristics of the urban heat island during the harmattan and monsoon in Akure, Nigeria. Eight Conferences on the Urban Environment. AMS 89th Annual Meeting, 11 – 15 January, 2009, Phoenix, AZ. Paper JP4.6
- Fujibe, F., (2009). Detection of Urban Warming in Recent Temperature Trends in Japan. *International Journal of Climatology*. 29(12) pp 1811-1822. DOI: 10.1002/joc.1822
- Ifatimehin, O.O., (2007). An Assessment of Urban Heat Island of Lokoja Town and Surroundings Using Landsat ETM data. *FUTY Journal of the Environment*, 2(1): 100-108.
- Ifatimehin, O.O. and M.E. Ufuah, (2007). An Analysis of Urban Expansion and Loss of Vegetation Cover in Lokoja, Using GIS Techniques. *Zaria Geographer*, 16(2) (in press).
- National Population Commission, *Federal Republic of Nigeria Official Gazette* 24: (96), Federal Government of Nigeria, (2007).
- Obasanjo O.T and Francis Martina , (2015). Quality of Intra-Urban Passenger Bus Services in Kaduna Metropolis, Nigeria. *International Journal of Traffic and Transportation Engineering* 2015, 4(1): 1-7 DOI: 10.5923/j.ijtte.20150401.01
- Odunuga, S., Badru, G., (2015). Land Cover Change, Land Surface Temperature, Surface Albedo and Topography in the Plateau Region of North-Central Nigeria. *Land*. 4, 300-324. doi:10.3390/land4020300

- Peng, S., Piao, S., Ciais, P., Friedlingstein, P., Otle, C., Bréon, F., Nan, H., Zhou, L., Myneni, R. B., (2012). Surface Urban Heat Island Across 419 Global Big Cities. *Environmental Science and Technology*. 46 (2), pp 696–703 DOI:10.1021/es2030438
- Umar, U. M., Kumar, J. S., (2014). Spatial and Temporal Changes of Urban Heat Island in Kano Metropolis, Nigeria. *International Journal of Research in Engineering Science and Technology* 1(2).
- United Nations (2014). World urbanization prospects: the 2014 revision highlights (ST/ESA/SER.A/352). UN Department of Economic and Social Affairs Population Division. See <http://esa.un.org/unpd/wup/>
- Zaharaddeen, I, Ibrahim.B and Zachariah, A. (2016). Estimation of Land Surface Temperature of Kaduna, Metropolis, Nigeria Using Landsat Images. *Science World Journal* Vol. 11 (No 3) 2016, ISSN 1597-6343
- Zhang, J., Wang, Y. and Li, Y. (2006). A C++ Program for Retrieving Land Surface Temperature from the Data of Landsat TM/ETM+ band 6. *Computers & Geosciences*, **32**, 1796-1805. <http://dx.doi.org/10.1016/j.cageo.2006.05.00>